A catalog of intermediate duration Type I X-ray bursts observed with the INTEGRAL satellite

Alizai, K.; Chenevez, J.; Brandt, S.; Lund, N.

Published in:
Monthly Notices of the Royal Astronomical Society

Link to article, DOI:
10.1093/mnras/staa831

Publication date:
2020

Document Version
Publisher's PDF, also known as Version of record

Monthly Notices
of the
ROYAL ASTRONOMICAL SOCIETY

MNRAS **494,** 2509–2522 (2020)
Advance Access publication 2020 March 28

doi:10.1093/mnras/staa831

A catalogue of intermediate-duration Type I X-ray bursts observed with the *INTEGRAL* satellite

K. Alizai ,★ J. Chenevez,★ S. Brandt and N. Lund

National Space Institute, Technical University of Denmark, DK-2800 Kongens Lyngby, Denmark

Accepted 2020 March 20. Received 2020 March 20; in original form 2020 January 23

ABSTRACT

We present a catalogue of long-duration bursts observed with the Joint European X-ray Monitor and IBIS/ISGRI instruments onboard the *INTEGRAL* satellite. The 14 bursts have e-folding times ranging from 55 s to ≈17 min, and are therefore classified as intermediate-duration bursts, caused by the ignition of an unusually thick helium layer. Though seven events have already been reported in literature, we have systematically reanalysed the whole sample. We find three new photospheric radius expansion bursts, which are not reported in the literature, allowing us to provide a new estimate of the distances to these sources. We apply the enhanced persistent emission method (also known as the f_a method) on sources with detectable persistent emission prior to a burst, in order to follow the evolution of the accretion rate during the burst. Although we do not get significantly better fits, the evolution of the f_a factor shows an indicative behaviour, which we discuss.

Key words: stars: neutron – X-rays: binaries – X-rays: bursts.

1 INTRODUCTION

More than 110 X-ray bursters have been identified in the Milky Way[1] since the first thermonuclear X-ray bursts were observed in 1975 (Grindlay et al. 1976; Swank et al. 1977). These are a subclass of X-ray binaries composed of a weakly magnetized neutron star, which accretes matter (hydrogen and/or helium) through the Roche lobe overflow from an orbiting lower mass companion star. In the most common scenario, the accumulated stellar matter on the surface of the neutron star forms an upper layer of hydrogen, which, due to the high temperature and density, steadily burns through thermonuclear fusion into a sublayer of helium (Hansen & van Horn 1975). For some accretion rates, the burning layer reaches a critical thickness above which the nuclear reactions become unstable at temperatures exceeding 20 million K.

Depending on their duration, X-ray bursts are divided into the following three groups:

(i) The most common X-ray bursts (≈99 per cent) have recurrence times of a few hours. They are caused by the ignition of either a pure helium (≈1 m thick) layer or a mixed helium and hydrogen layer. Mostly depending on the thickness of the burning layer, the duration of the bursts can be from tens to a few hundreds of seconds (Maraschi & Cavaliere 1977; Lewin, van Paradijs & Taam 1993; Strohmayer & Bildsten 2006; Galloway & Keek 2017); >8000 bursts have been recorded in the past 50 yr (Galloway, in't Zand & Chenevez, *Multi-INstrument Burst ARchive (MINBAR),* in prep). For the pure helium bursts, the luminosity can often reach the local Eddington limit, causing a photospheric radius expansion (PRE) burst. The accretion luminosity of the sources, prior to a burst, is around a few per cent of the Eddington luminosity.

(ii) X-ray bursts with durations of few minutes up to a few tens of minutes are called intermediate-duration bursts. They have recurrence time of weeks to months and are due to the ignition of a thick (10–100 m) layer of helium. Most commonly, the accretion luminosity prior to an intermediate-duration X-ray burst is ≈1 per cent of the Eddington limit, GX 17+2 being the exception (Kuulkers et al. 1997, 2002). To date, 70 of these bursts have been observed.

(iii) The rarest X-ray bursts (27 to date) have durations of several hours up to 1 d and are called superbursts (Cornelisse et al. 2000; Kuulkers 2004). Simulations indicate that superbursts have recurrence times of a year (Keek et al. 2008) and have an energy output 10^3 times greater than that of regular bursts. Superbursts occur for a wide range of accretion rates and are usually sub-Eddington (although precursors to superbursts do reach the Eddington limit). They are thought to be due to an ignition of a deep carbon layer.
To date, we have only observed a single superburst with the *INTEGRAL*/JEM-X instrument from SAX J1747.0-2853 on 2011 February 11 (Chenevez et al. 2011) (to be published in a separate paper).

The BeppoSAX Wide Field Camera instrument (Jager et al. 1997) and the Joint European X-ray Monitor (JEM-X) on the *INTEGRAL* satellite are, because of their large field of view (FOV)

★ E-mail: kha@space.dtu.dk (KA); jerome@space.dtu.dk (JC)
[1] https://personal.sron.nl/jeanz/bursterlist.html (last update: 2018 April 26).

Table 1. List of all long X-ray bursts investigated in this study.

Source	Detection date	MJD	Revolution/ScW	Off-axis(^{o})	Instrument(s)	Reference
SLX 1737-282	2004-03-09	53073.72296	0171/75	5.05	JEM-X 1	Falanga et al. (2008)
SLX 1735-269	2004-04-13	53108.20530	0183/11	N/A	IBIS/ISGRI	Sguera, Bazzano & Bird (2007)
GX 3+1	2004-08-31	53248.78751	0230/09	2.46	JEM-X 1	Chenevez et al. (2006)
SLX 1737-282	2005-04-11	53471.35022	0304/61-62	1.72/1.74	JEM-X 1	Falanga et al. (2008)
AX J1754.2-2754	2005-04-16	53476.92472	0306/50	1.85	JEM-X 1	Chelovekov & Grebenev (2007)
IGR J17254-3257	2006-10-01	54009.30180	0484/42-43	3.66/2.76	JEM-X 1	Chenevez et al. (2007)
SLX 1737-282	2007-04-02	54192.24886	0545/48	3.73	JEM-X 1	Falanga et al. (2008)
GX 17+2	2012-03-25	56011.77901	1153/116	2.03	JEM-X 1 and 2	This work
GX 17+2	2012-08-21	56160.00084	1203/49	2.93	JEM-X 1 and 2	This work
SLX 1744-299	2013-04-06	56388.46546	1279/69	2.66	JEM-X 1 and 2	This work
SLX 1744-299	2015-02-27	57080.41900	1512/58	2.42	JEM-X 1 and 2	This work
SLX 1744-299	2016-03-07	57454.43753	1653/16	3.41	JEM-X 1 and 2	This work
AX J1754.2-2754	2017-03-12	57824.16536	1792/17	1.17	JEM-X 1 and 2	This work
SAX J1712.6-3739	2018-02-13	58169.96485	1922/13	1.29	JEM-X 1 and 2	This work

Table 2. Properties of the bursts studied in this paper.

Source	Obs. date	Bol. $F_{\rm peak}$[a]	e-folding time (s)	d (kpc)	$E_{\rm b}$[b]	$y_{\rm b}$[c]
AX J1754.2-2754	2005-04-16	5.10 ± 0.20	56 ± 5	7.1	1.65 ± 0.06	1.1 ± 0.2
AX J1754.2-2754	2017-03-12	4.9 ± 0.25	113 ± 13	7.1	3.2 ± 0.1	2.1 ± 0.2
GX 3+1	2004-08-31	3.5 ± 0.30	1011 ± 140	5	6.3 ± 0.3	4.1 ± 0.2
GX 17+2	2012-03-25	5.0 ± 0.15	576 ± 120	8	17 ± 4.0	11 ± 3.0
GX 17+2	2012-08-21	5.7 ± 0.20	347 ± 90	8	16 ± 4.0	10 ± 3.0
IGR J17254-3257	2006-10-01	1.5 ± 0.10	182 ± 50	14.5	9 ± 3	5.9 ± 2
SAX J1712.6-3739	2018-02-20	8.32 ± 0.20	86 ± 10	7	4.9 ± 0.3	3.2 ± 0.2
SLX 1737-282	2004-03-09	6.2 ± 0.10	230 ± 80	7.3	11 ± 1.0	7.2 ± 0.7
SLX 1737-282	2005-04-11	5.7 ± 0.25	245 ± 20	7.3	11 ± 1.0	7.2 ± 0.7
SLX 1737-282	2007-04-02	5.1 ± 0.15	195 ± 15	7.3	9.1 ± 1	5.9 ± 0.7
SLX 1744-299	2013-04-06	4.3 ± 0.20	76 ± 12	8.5	2.8 ± 0.2	1.8 ± 0.1
SLX 1744-299	2015-02-27	3.0 ± 0.10	172 ± 30	8.5	4.8 ± 0.6	3.1 ± 0.4
SLX 1744-299	2016-03-07	4.0 ± 0.15	55 ± 10	8.5	1.90 ± 0.3	1.2 ± 0.2

Note. [a]($\times 10^{-8}$ erg cm^{-2} s^{-1}).
[b]($\times 10^{40}$ erg).
[c]10^9 g$*$cm^{-2}.

(0.3 per cent of the sky for *INTEGRAL*/JEM-X and 8 per cent for BeppoSAX/WFC), the utmost instruments for detecting long-duration bursts. These are both coded-mask telescopes that image by blocking radiation in a known pattern casting a 'shadowgram' on the detector plane, which is then reconstructed to an image (in't Zand 1992).

Because of their long duration, superbursts can also be detected by instruments that do not have a particularly large FOV, but that scan the sky on regular intervals. Such instruments are the ISS/MAXI and the RXTE/ASM that scan > 80 per cent of the sky every 1.5 h.

There are other instruments in orbit that have a large FOV, but their band passes do not cover the relevant energy range for X-ray bursts and at most these devices can detect the hard X-rays from the bursts, which are evident in the beginning of the bursts, but fade out quickly. The peak effective temperature of an X-ray burst, derived from the spectroscopy, is around 2–3 keV. This indicates that the energy spectrum peaks at 6–9 keV. Amongst the wide-field cameras most preferable for the hardest photons are IBIS/ISGRI detector onboard *INTEGRAL* (18 keV–10 MeV) (Chernyakova et al. 2015), the imaging Burst Alert telescope (BAT) onboard the *Swift* observatory (15–150 keV) (Markwardt et al. 2007) and the *Fermi* Gamma-ray Burst Monitor (GBM; 8 keV–1 MeV) (Band & Ferrara 2009).

Thermonuclear X-ray bursts are, in general, interesting for observers, because they can improve our understanding of the fuel composition and accretion rate, as well as the neutron star spin, mass, and radius (Strohmayer & Bildsten 2006; Heger et al. 2007; Cumming & Bildsten 2000; 2001; Cumming & Macbeth 2004; Fujimoto, Hanawa & Miyaji 1981). The rare intermediate-duration bursts are particularly interesting, because they can be used to probe the thermal properties of the neutron star interior, as they occur deep in the neutron star envelope and their ignition is therefore sensitive to the thermal profile of the crust and the core of the neutron star (Cumming et al. 2006). Different numerical models have been used to understand the burning physics, ignition conditions, and energy release of intermediate-duration bursts, but the model predictions have not been compared to observations in a sufficient degree, partly because of the lack of a statistically significant sample (in't Zand et al. 2005; Falanga et al. 2008; Kuulkers et al. 2010).

In this paper, we present intermediate-duration X-ray bursts detected with instruments onboard the *INTEGRAL* satellite. In Section 2, we give an overview of the *INTEGRAL*/JEM-X instrument and the data analysis software. In Section 3, we present the data sample used for this study and give an overview of the data from literature, which has been reused for this study. In Section 4, we present our data analysis methodology. Section 5 is

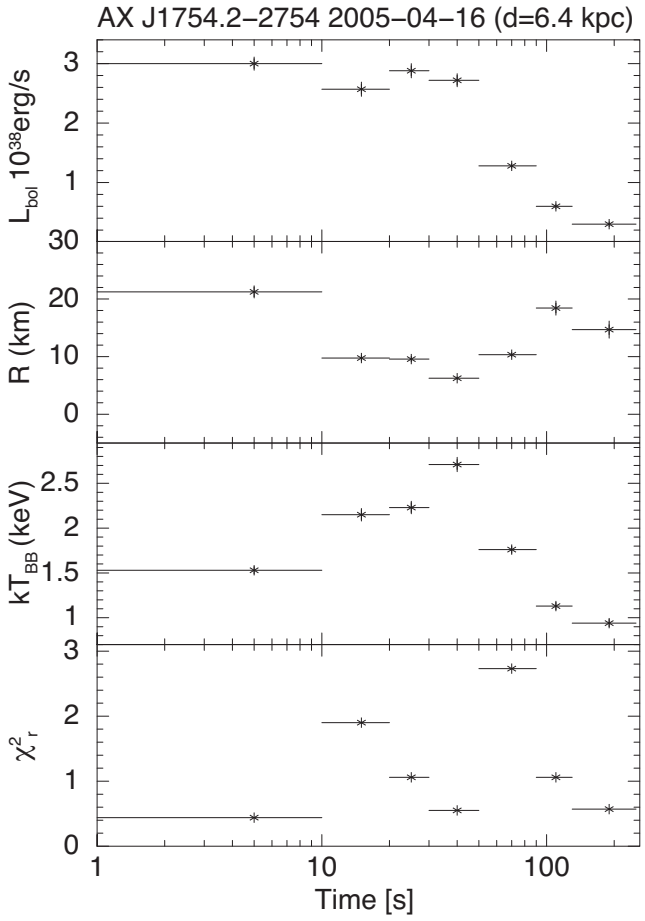

Figure 1. AX J1754.2-2754/2005-04-16: time-resolved spectroscopy.

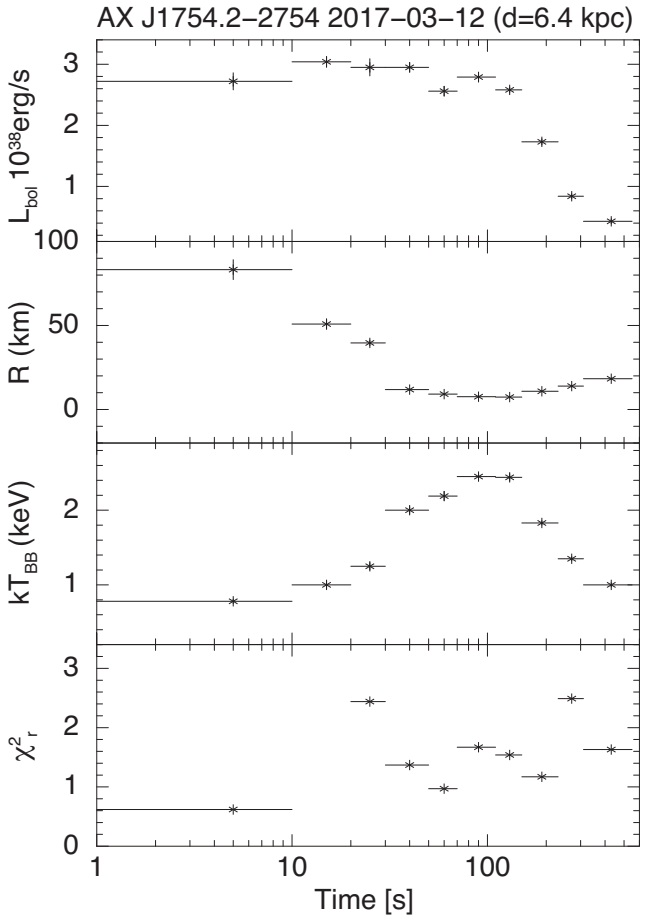

Figure 2. AX J1754.2-2754/2017-03-12: time-resolved spectroscopy.

dedicated to a presentation of our results. In Section 6, we provide a discussion of our results and the physics that can be done with a catalogue like ours. In Section 7, we provide a summary and a conclusion.

2 INSTRUMENTATION AND DATA ANALYSIS SOFTWARE

The *INTErnational Gamma-Ray Astrophysics Laboratory* (*INTEGRAL*) was launched into orbit in 2002 by the European Space Agency (ESA). *INTEGRAL* is a dedicated 20 keV–10 MeV gamma-ray observatory with secondary instruments that have the capability of source monitoring at X-rays (JEM-X, 3–35 keV) and in the optical range of the electromagnetic spectrum (OMC, 500–600 nm). The primary instruments of the *INTEGRAL* payload are the SPECTROMETER (SPI; 15 keV–10 MeV) and the IMAGER (IBIS; 20 keV–10 MeV); the latter consists of two detector planes: ISGRI and PICsIT.

The instruments of interest for our study are JEM-X and the ISGRI detector. JEM-X consists of two twin coded-mask telescopes, which are co-aligned with the other instruments on *INTEGRAL*. JEM-X has a useful FOV of 5.5° in diameter, 3 arcmin angular resolution, and an energy resolution of $\Delta E/E = 47$ per cent $(\mathrm{E/1\ keV})^{-1/2}$. The energy range of JEM-X is 3–35 keV (Lund et al. 2003; Kuulkers 2011). ISGRI is the top layer of the IBIS instrument. It has a collecting area of 2600 cm^2, has an energy resolution of 8 per cent@100 keV, angular resolution of 12 arcmin FWHM, FOV of 8.3° × 8.0° (fully coded), and an energy of 15–1000 keV (with a maximum effective area between 20 and 100 keV) (Savchenko et al. 2018).

A single pointing of *INTEGRAL* is called a science window (ScW). For this study, we have used the standard offline Science Analysis (OSA) software version 11. OSA11 for JEM-X has 11 scientific levels, through which JEM-X data are corrected for instrument effects and deadtime. Furthermore, good time intervals are created to be used for image reconstruction and spectra extraction (Westergaard et al. 2003).

3 OBSERVATIONS

The observations included in this study were carried out over the span of 14 yr (2004–2018). So far, 15 intermediate-duration bursts have been serendipitously detected from 8 sources by *INTEGRAL*, since its launch. 11 bursts are only detected by JEM-X, three bursts are detected by both JEM-X and IBIS/ISGRI, and one burst is detected by IBIS/ISGRI alone. Nine of the bursts have been previously published in peer-reviewed papers or in Astronomer's Telegrams (ATel). Table 1 shows a list of the bursts included in this study. We present light curves and time-resolved spectral analyses (TRSAs) for 14 of the 15 intermediate-duration bursts detected by *INTEGRAL*, where we have redone the TRSA for 5 bursts with different time intervals and different

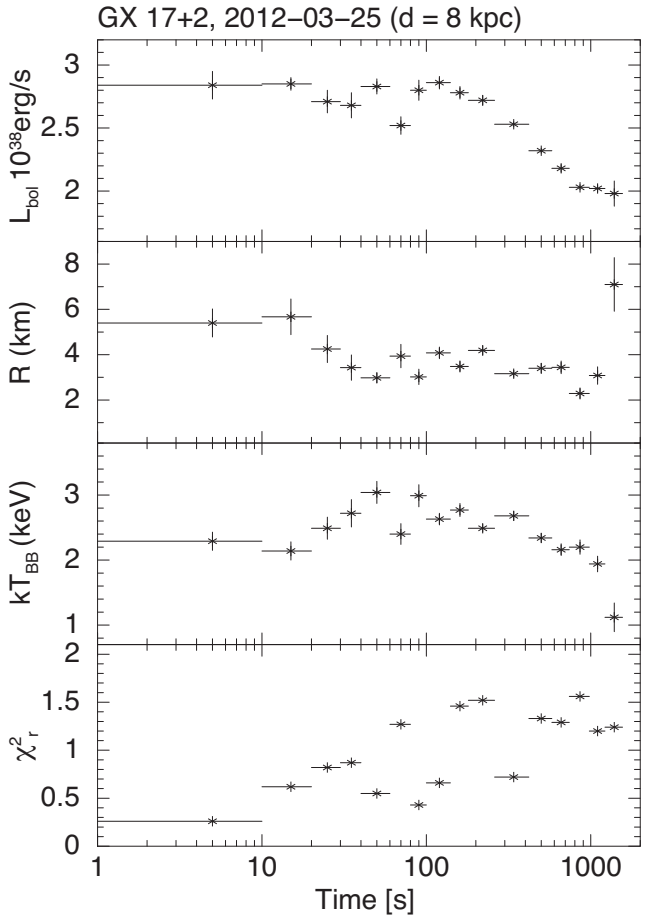

Figure 3. GX 17+2/2012-03-25: time-resolved spectroscopy.

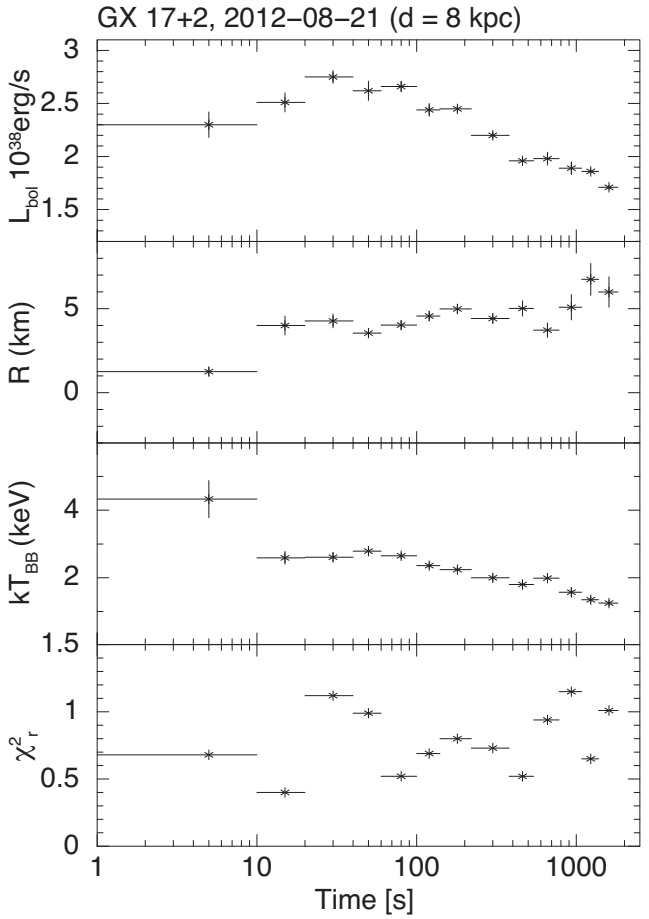

Figure 4. GX 17+2/2012-08-21: time-resolved spectroscopy.

models relative to those published in the literature. The missing burst is from the source SLX 1735-269 detected on 15th of September, 2003, during which JEM-X was running in restricted mode (Molkov et al. 2005), a data format that is not supported by OSA 11.

All uncertainties reported in this paper are at 1σ.

4 ANALYSIS OF THE DATA

The JEM-X light curves can be extracted for several different energy bands in the detector energy range of 3–35 keV. Since most of photons from a bursting source have energies below 25 keV, we extract light curves between 3 and 25 keV. We fit the light curves with an exponential function (and a constant component for the noise), and quote the e-folding time as τ.

Due to the relatively small effective area of JEM-X (60–100 cm^2, E-depending), we use only eight energy bins to extract the spectra. The choice of time intervals for the TRSA is based on the consideration of having a minimum of 1200 counts per spectrum in our TRSA. This minimum is chosen to ensure enough counts in each of the energy bins, as a burst progresses and its spectrum becomes softer. Therefore, the length of the intervals is increased through the evolution of the burst.

The spectral analysis is performed with the XSPEC software (Arnaud 1996). Because of the low number of energy bins, we use simple fitting models in an attempt to have the highest number of degrees of freedom (dof) as possible (dof = 4 for all the spectra included in this study).

We set the solar abundance and the photoionization cross-section to WILM and VERN (in XSPEC syntax), respectively. We then use the model TBABS as our absorption model. We quote the absorption column from literature and freeze the value. The persistent emission of the sources is only detected for 7 out of the 14 bursts we have analysed. We model the persistent emission with a simple power law (PO in XSPEC syntax) for five of the seven cases. For the remaining two cases, we model their persistent emission with the XSPEC model CUTOFFP, which is a power law with high-energy exponential rolloff. The models are chosen so they give the best fit for our data. We then include the model for the persistent emission in the model for the burst itself, but we freeze all model parameters from the persistent emission model. We assume that the bursts themselves emit as a blackbody reasonably well and use the XSPEC model BBODYRAD to fit the burst emission component. For bursts without any detectable persistent emission, we fit the spectra with only the blackbody model BBODYRAD.

The distances used in this study are either quoted from the literature or estimated from PRE bursts. We have looked through the Data Release 2 of the *Global Astrometric Interferometer for Astrophysics* (*Gaia*) for distances measured to the sources of interest for our study; since most of our sources are in crowded regions of the sky, we do not get any reliable parallax for them and we can therefore not quote any *Gaia* distances (Brown 2018). We use the source distances as fixed values without considering their uncertainties.

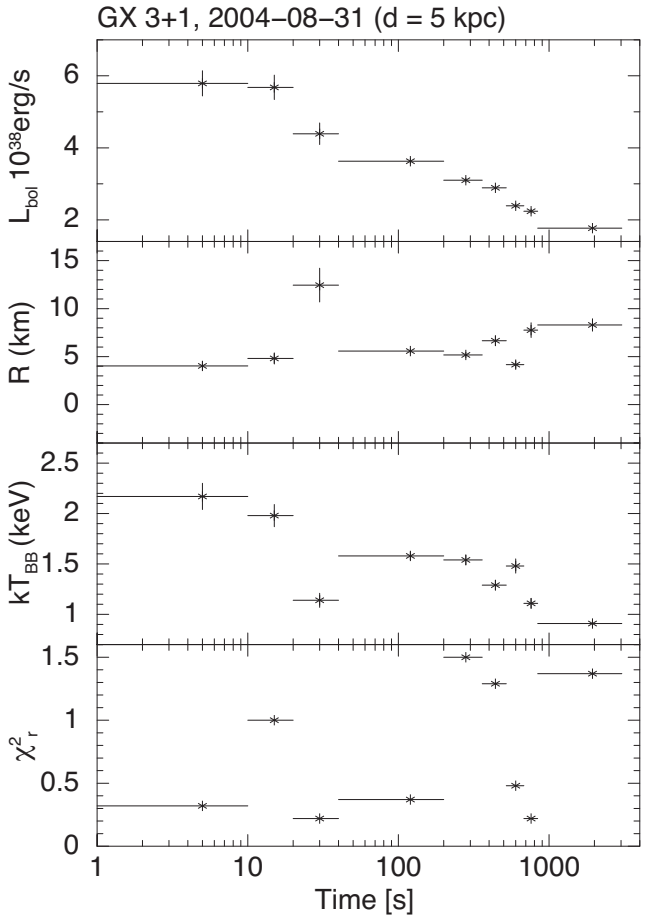

Figure 5. GX 3+1: time-resolved spectroscopy.

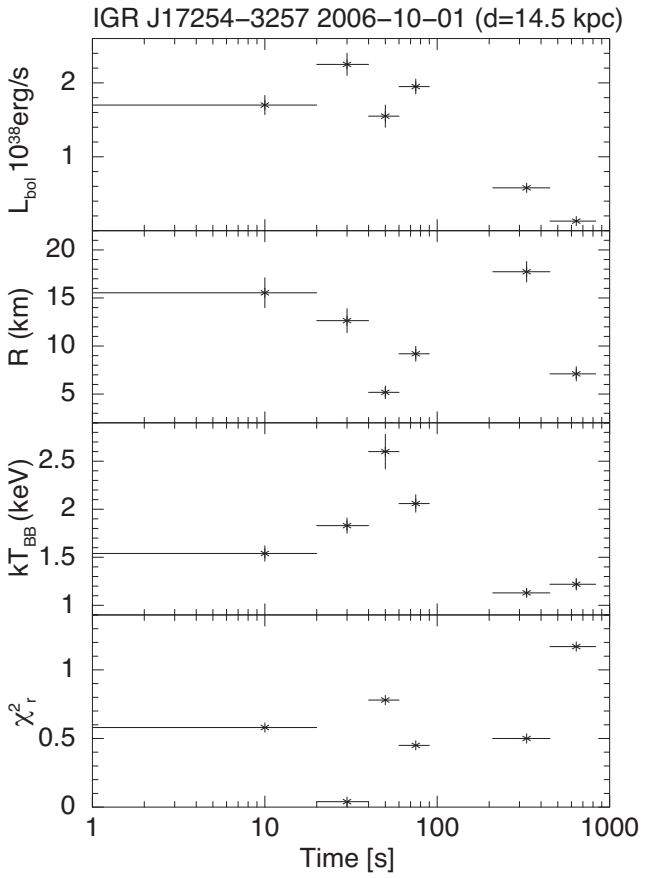

Figure 6. IGR J17254-3257: time-resolved spectroscopy.

5 RESULTS

5.1 Burst light curves

We present the count-rate light curves of the 14 X-ray bursts detected by *INTEGRAL* in Fig. A1 (Appendix A). Figs A1(a)–(m) show the JEM-X light curves (3–25 keV), where the bottom panel of Figs A1(h)–(j) shows the IBIS/ISGRI light curves (20–60 keV) of the bursts. Fig. A1(n) shows IBIS/ISGRI light curve (20–60 keV) of the 2004 burst from SLX 1735-269 detected only by IBIS/ISGRI. The e-folding times, obtained from fitting the count-rate light curves with an exponential function, for 13 bursts (the only IBIS/ISGRI burst not included) range from 55 ± 10 s up to 1011 ± 140 s. The e-folding times are listed in Table 2. We observe the rise phase of 12 bursts in our sample. The two-phase X-ray burst from GX 3+1 is the only burst in our sample with a fast rise time (<2 s), the remaining bursts all exhibit long rise times (>10 s). We choose to plot each light curve with a time bin that reduces noise as much as possible.

5.2 Bursts from AX J1754.2-2754

The first observation of the source AX J1754.2-2754 was made by the *ASCA* observatory on 1999 October 2–3 (Sakano et al. 2002), but it was not until 2005 that the nature of the compact object could be determined, when the first burst was detected (Chelovekov & Grebenev 2007). The interstellar absorption of the source is found to be $N_{\rm H} = 2.0 \times 10^{22}$ cm^{-2} (Sakano et al. 2002).

5.2.1 2005 April 16

This burst was already published by Chelovekov & Grebenev (2007). Based on this burst, the source was classified as an X-ray burster. Furthermore, two distances were estimated to the source, since it clearly was a PRE burst. The two distances estimated to the source were $d = 6.6 \pm 0.3$ kpc (for hydrogen atmosphere) and $d = 9.2 \pm 0.4$ kpc (for helium atmosphere). For the latter, the empirically obtained Eddington luminosity $L_{\rm Eddington} = 3.8 \times 10^{38}$ erg s^{-1} was used (Kuulkers et al. 2003). We have reestimated the distance to the source using the theoretical value of 3.0×10^{38} erg s^{-1} for the He Eddington luminosity (assuming a 1.4 $M_\odot$ neutron star with $R_{\rm NS} = 10$ km), and derive a distance of $d = 7.01 \pm 0.2$ kpc, at a peak flux of 5.2×10^{-8} erg cm^{-2} s^{-1} (see Fig. 1).

5.2.2 2017 March 12

The 2017 burst from AX J1754.2-2754 is the longest burst detected from the source. Like the burst from 2005, the 2017 burst is also a PRE burst. We estimate the distance to the source based on the peak flux of this burst also and get 7.2 kpc. With the peak flux of 4.9×10^{-8} erg cm^{-2} s^{-1}, the distance is derived (using 3.0×10^{38} erg s^{-1} as the Eddington luminosity). This is the most recent burst detected from AX J1754.2-2754 (see Fig. 2).

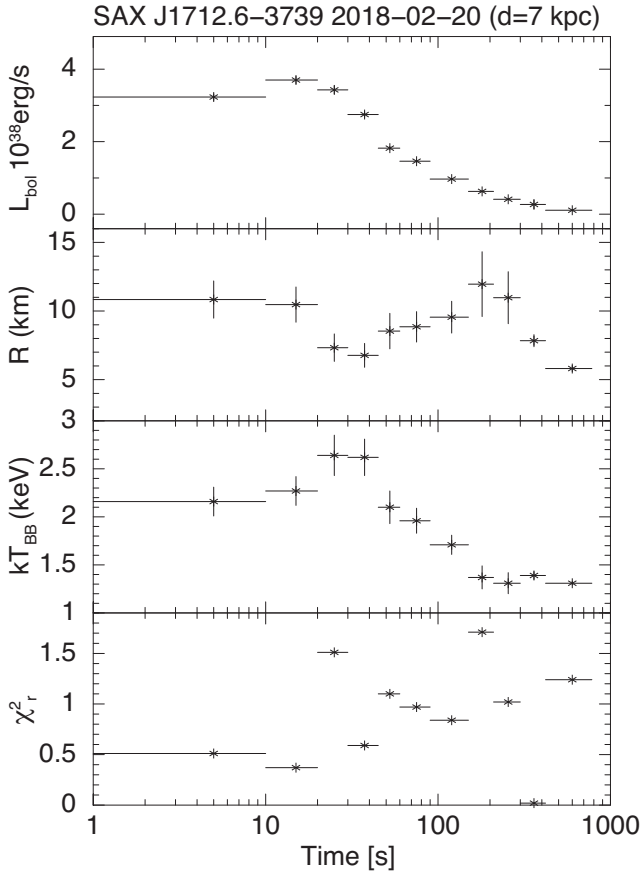

Figure 7. SAX J1712.6-3739: time-resolved spectroscopy.

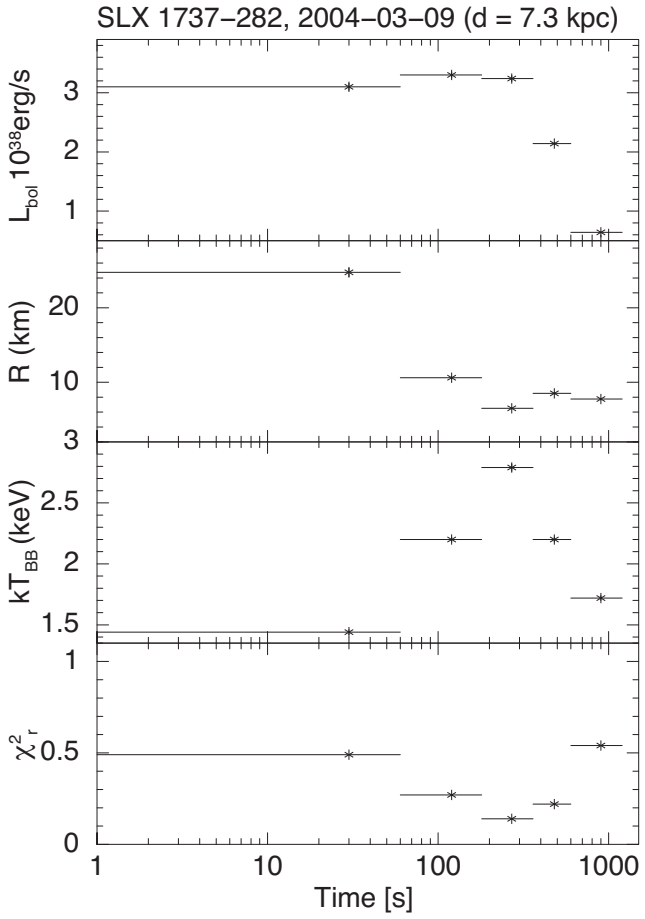

Figure 8. SLX 1737-282: time-resolved spectroscopy.

5.3 Bursts from GX 17+2

The bright persistent source GX 17+2 is only one of two Z-sources that have showed X-ray bursts, the other being Cygnus X-2. GX 17+2 accretes matter close to the Eddington limit, and has shown short-, intermediate X-ray bursts, and superbursts. A distance of 12 kpc has been derived for the source from five PRE bursts (Kuulkers et al. 2002; in't Zand, Cornelisse & Cumming 2004). The JEM-X instrument has detected two intermediate-duration X-ray bursts from GX 17+2. Both of them occurred in 2012 almost 5 months apart.

5.3.1 2012 March 25

The first intermediate burst from GX 17+2 was detected on 2012 March 25. The burst onset occurs 120 s after the start of the ScW. The tail of the burst seems to continue even after it is not in the FOV of the instrument. The peak flux of the burst is 5.0×10^{-8} erg cm^{-2} s^{-1}, which corresponds to a peak luminosity of 8.62×10^{38} erg s^{-1}, which is well above the Eddington luminosity. We can instead use the distance calculated by Kuulkers et al. (2002), where they considered the gravitational redshift effects and estimated a distance of 8 kpc. The results presented in Fig. 3 are calculated assuming a distance of 8 kpc. The blackbody temperature for most of the burst is above 2 keV. Notice the significant decrease in the temperature at the last data point.

5.3.2 2012 August 21

The second JEM-X intermediate burst from GX 17+2 was detected on 2012 August 21. The peak of the burst is not detected, since the source is not in the FOV at the time. We see the tail of the burst from the start of the ScW and it continues to decrease in flux throughout the entire ScW. As for the March burst, the blackbody temperature is above 2 keV for the large part of the burst and we first notice a significant decrease in the latter part of the burst (see Fig. 4).

5.4 Burst from GX 3+1

GX 3+1 is a persistent atoll source, which is always in the soft (banana) state (Seifina & Titarchuk 2012). The source is a well-known burster that has shown regular bursts and a superburst (Kuulkers 2002). *INTEGRAL*/JEM-X detected an unusual burst from GX 3+1 on 2004 August 31. A TRSA of the burst was presented by Chenevez et al. (2006), which clearly showed spectral softening. The unusual aspects of the burst from 2004 are the initial spike and the prolonged tail, which continues for more than 2000 s. Chenevez et al. (2006) used a two-component spectral analysis for both the persistent emission and burst emission. The model used contained a blackbody (BB) component for the thermal emission and the power-law (PO) component for the Comptonized photons.

We have reanalysed the burst using also a two-component spectral model, but we use two different models for the persistent emission and the burst emission, respectively. We use the DISKBB model

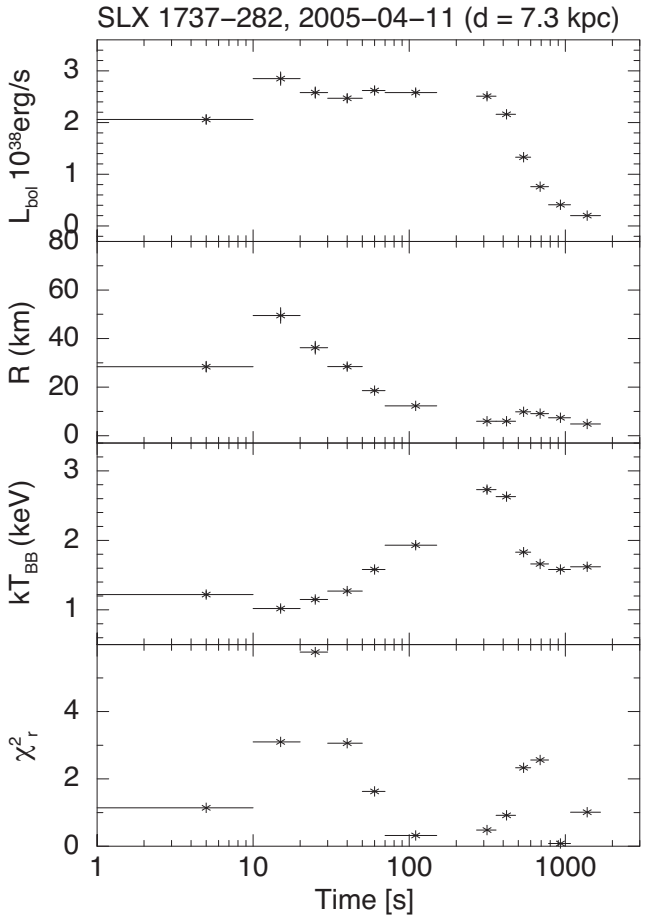

Figure 9. SLX 1737-282: time-resolved spectroscopy.

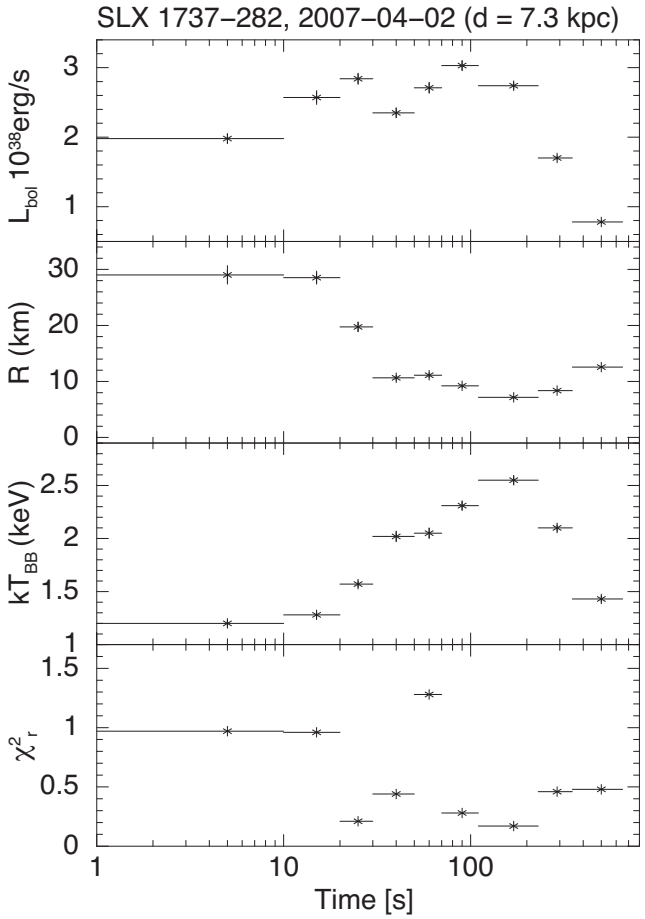

Figure 10. SLX 1737-282: time-resolved spectroscopy.

(with the absorption model TBABS) from XSPEC for the persistent emission, where we assume an accretion disc consisting of multiple blackbody components. For the burst emission, we use an absorbed blackbody (BBODYRAD). We use $N_{\rm H} = 1.6 \times 10^{22}$ atoms cm^{-2} derived by Oosterbroek et al. (2001). For the model parameters and other burst parameters of the whole burst sample, see Table 2. Although we do not use the same models as in the original publication, we do get the same parameter values (see Fig. 5). However, if we use a PO to model the persistent emission, we get poorer fits than we do with the DISKBB model.

5.5 Burst from IGR J17254-3257

IGR J17254-3257 was discovered by *INTEGRAL* in 2003 in the Galactic Centre hard X-ray survey (Walter, Bodaghee & Barlow 2004; Markwardt et al. 2008). To date, only two X-ray bursts have been detected from this source. The first X-ray burst was an ordinary one, detected on 2004 February 17. The second burst was detected on 2006 October 1 and was identified as an intermediate burst (Chenevez et al. 2007). We present the first ever TRSA of the second burst from this source in Fig. 6. There is a data gap of 2 min during the burst, caused by the slew of the instrument. We use 14.5 kpc as the upper limit of the distance, derived by using 3.8×10^{38} erg s^{-1}. We use $N_{\rm H} = 1.79 \times 10^{22}$ cm^{-2} that was obtained as one of the best-fitting parameters by Chenevez et al. (2007) using the joined spectrum of pn/MOS1/JEM-X/ISGRI. The source is too weak to be detected prior to the burst, which prevents us from using the two-component method, and instead we fit the burst spectra with an absorbed blackbody.

5.6 Burst from SAX J1712.6-3739

SAX J1712.6-3739 source was discovered by BeppoSAX in 1999 (in't Zand et al. 1999), and it has been categorized as a persistent source since 2001. Immediately after its discovery, the source showed two regular Type I X-ray bursts. Based on these first X-ray bursts, the distance to the source was estimated to 7 kpc (in't Zand et al. 1999). To date, the source have shown several intermediate bursts and a single superburst-like flare, detected with the BAT onboard the *Swift* satellite. The only intermediate X-ray burst, detected by JEM-X, occurred on 2018 February 20.

We present the TRSA in Fig. 7. The spectra are fitted using a column density $N_{\rm H} = 2 \times 10^{22}$ (in't Zand et al. 1999). Since the burst does not show a clear PRE, we assume the distance of 7 kpc. The burst reaches the peak flux of $F_{\rm peak} = (1.1 \pm 0.2) \times 10^{-7}$, which gives us a peak luminosity of $L_{\rm peak} = (6.45 \pm 1.17) \times 10^{38}$, well above the local Eddington luminosity. Using the peak flux, we derive an upper limit for the distance by fixing the Eddington luminosity to $L_{\rm Edd} = 3.0 \times 10^{38}$. The result is a distance of $d = 4.77 \pm 0.8$ kpc, but we refrain from using this distance in our TRSA, since it is an upper limit.

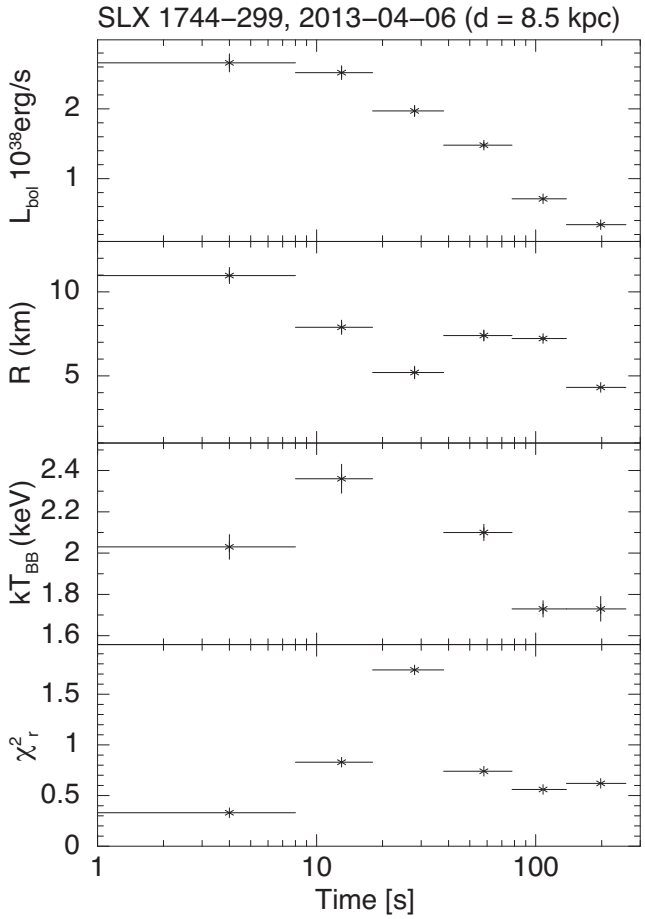

Figure 11. SLX 1744-299: time-resolved spectroscopy.

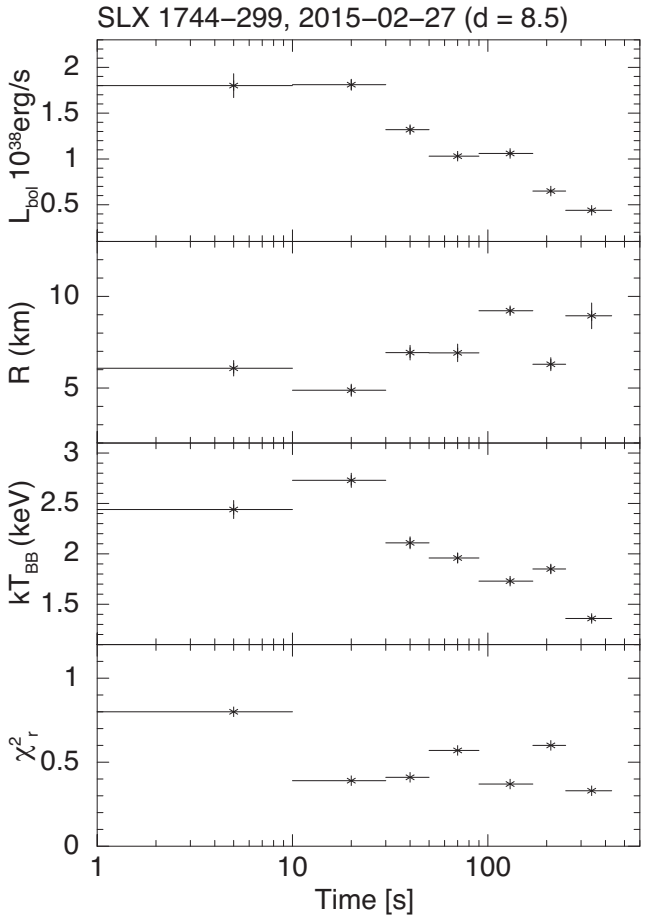

Figure 12. SLX 1744-299: time-resolved spectroscopy.

5.7 Bursts from SLX 1737-282

SLX 1737-282 was discovered in 1985 with the *Spacelab – 2* (Skinner et al. 1987). The source has since been categorized as a low persistent source. Only intermediate X-ray bursts have been observed from the source (four to date). Falanga et al. (2008) published their results on the investigation of the three intermediate bursts, observed with JEM-X, in 2008, where they confirmed one of the three to be a PRE burst. We have reanalysed the data from the three bursts, where we have increased the number of spectra extracted for each burst. The column density in the direction of the source is fixed to $N_{\rm H} = 1.9 \times 10^{22}$ for all our spectral fits. We assume a distance of 7.3 kpc, which was observationally obtained by Falanga et al. (2008).

5.7.1 2004 March 9

This is the first burst detected by JEM-X from the source, and it is also the burst with the shortest e-folding time of the three. Falanga et al. (2008) did not identify this burst as a PRE, but from our spectral analysis, we see an anticorrelation between the blackbody norm and the blackbody temperature $kT_{\rm BB}$, which is indicative of a PRE. We show our TRSA in Fig. 8.

5.7.2 2005 April 11

The burst with the longest e-folding time of the three was detected in 2005. This burst was identified by Falanga et al. (2008) as a PRE, and was used to estimate the 7.3 kpc distance. Compared to their analysis, we have extracted 12 spectra of the burst instead of 8. This gives us a better detailed picture of the burst itself, where we have been able to resolve the start of the expansion phase, indicated by a decrease in $kT_{\rm BB}$ at the start of the burst (see Fig. 9).

5.7.3 2007 April 2

Just as for the first burst, this last burst from the SLX 1737-282 was not identified as a PRE. However, our spectral analysis again shows an anticorrelation between the blackbody norm and $kT_{\rm BB}$ (see Fig. 10), indicating a PRE burst. To ensure that this anticorrelation between the norm and the blackbody temperature is real, we fixed the temperature at several different intermediate values and we saw that the quality of our fits deteriorated every time, indicating that a variable temperature and radius are required to fit the data.

5.8 Bursts from SLX 1744-299

SLX 1744-299 was discovered with *Spacelab – 2* in 1987 (Pavlinsky, Grebenev & Sunyaev 1994). The source is close to another

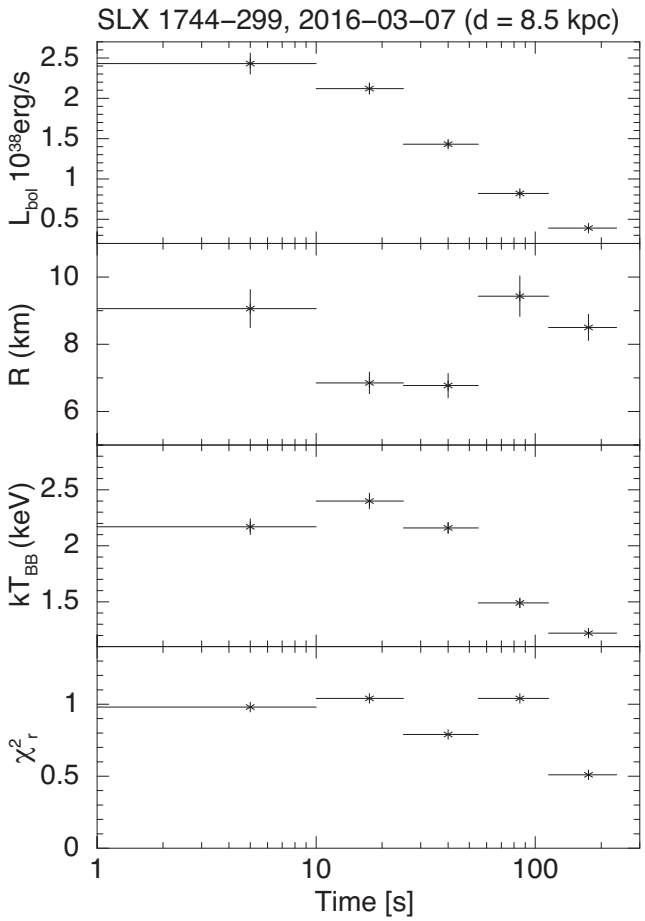

Figure 13. SLX 1744-299: time-resolved spectroscopy.

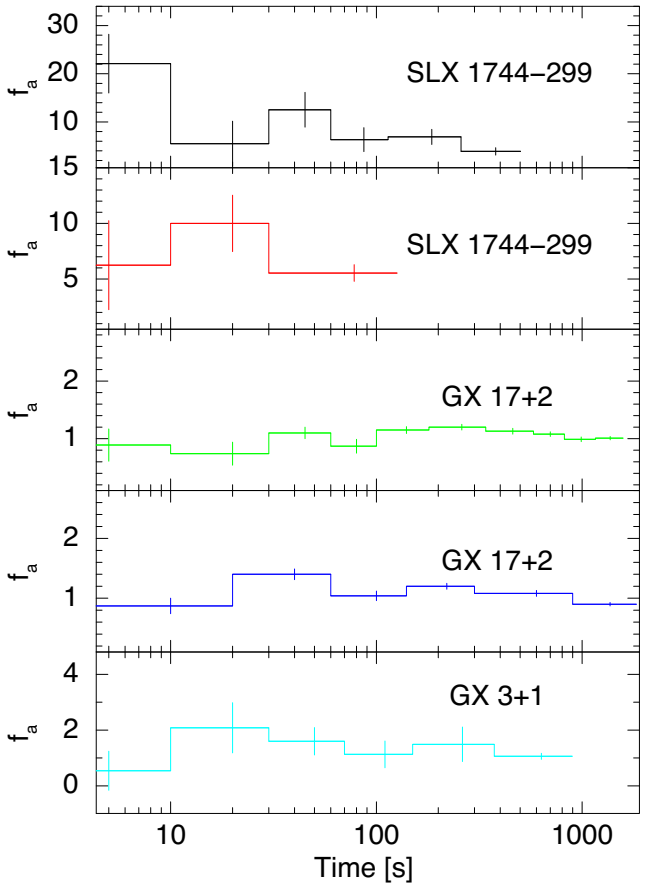

Figure 14. Evolution of the f_a factor.

burster SLX 1744-300 on the sky; it was therefore only possible to measure a combined flux of the two sources with all the non-focusing telescopes. The only measurement of the fluxes of both the sources was made on the basis of a 2004 *XMM–Newton* observation, which resolved both the sources, and found a ratio of 2.8/1.0 between SLX 1744-299 and SLX 1744-300. in't Zand, Jonker & Markwardt (2004) categorized this source as a UCXB candidate, based on the apparent low accretion rate (i.e. slow recurrence of bursts). Nevertheless, it is interesting to note that none of the bursts (six intermediate bursts to date) detected from SLX 1744-299 show a PRE, even though the accreted matter is thought to be He.

We present TRSA of three intermediate bursts from SLX 1744-299. We assume a column density of $N_{\rm H} = 4.34 \times 10^{22}$ cm^{-2} and a distance to the source of 8.5 kpc, both the values obtained from *XMM–Newton* observations (Pavlinsky et al. 1994).

5.8.1 2013 April 6

Fig. 11 shows the TRSA of the first burst detected from this source. The effective duration of the burst is approximately ≈200 s, the peak flux is $F_{\rm peak} = (4.3 \pm 0.4) \times 10^{-8}$ erg cm^{-2} s^{-1}, and the peak blackbody temperature is $kT_{\rm BB} = 2.36 \pm 0.07$ keV (see Fig. 11).

5.8.2 2015 February 27

The onset of this burst occurs during the slew from one pointing to another. We therefore only see the tail of the burst, where the maximum flux registered is $F_{\rm max} = (2.5 \pm 0.2) \times 10^{-8}$, the maximum blackbody temperature is $kT_{\rm BB} = 2.73 \pm 0.08$ keV, and we have a lower limit for the effective duration of ≈300 s; see Fig. 12.

5.8.3 2016 March 7

This burst is the shortest of all the three, observed by JEM-X. The effective duration of this burst is ≈100 s, the peak blackbody temperature is $kT_{\rm BB} = 2.40 \pm 0.07$ keV, and a peak flux of $F_{\rm peak} = (3.8 \pm 0.15) \times 10^{-8}$; see Fig. 13.

The three bursts from SLX 1744-299 all show a peculiar 'shoulder' at around 60 per cent of the peak. This 'shoulder' is evident in all the light curves, where it actually occurs as a second peak in the third burst; see Fig. A1 (k, l, m). This 'shoulder' is also evident in the spectral analysis of the second burst, where the bolometric flux is constant over a period of ≈150 s; see Fig. 13. Furthermore, we have found that this 'shoulder' is evident in light curves from all the bursts, detected from this source.

6 DISCUSSION

6.1 Burst energetics

The duration of X-ray bursts is determined by the composition and thickness of the fuel layer. The total energy release is $E_b = F_p \times \tau(1 - e^{-T/\tau})$ (where we use e-folding times from Table 2 as τ, and T is the time when the burst intensity stays above 20 per cent of the peak), which is of the order of 10^{40}–10^{41} erg. Based on the observed E_b, we calculate an ignition depth for each of the bursts in our sample, using the formula $y_b = E_b(1 + z)/4\pi R^2 Q_{nuc}$. We use $Q_{nuc} = 1.6$ MeV per nucleon, which is the energy release for burning helium to iron group nuclei. Furthermore, we use $R = 10$ km (radius of the neutron star) and $z = 0.31$ (gravitational redshift), assuming a 1.4 $M_\odot$ neutron star. In general, the ignition column depths associated with intermediate bursts are of the order of 10^9–10^{10} g cm^{-2}, assuming a thick He.

The bolometric peak flux of each burst is obtained by taking the ratio of the count rate at the peak in 1 s light curve of the burst and the average count rate given in the spectrum of the time interval at the peak, and then multiplying this ratio by the bolometric flux obtained from spectroscopy of the spectrum at the peak.

We present y_b and Bol. F_{peak} for all the JEM-X bursts in Table 2.

All bursts detected by JEM-X exhibit the same characteristics as the intermediate bursts (i.e. E_b and y_b). We cannot conclude anything definitive about the nature of the only burst detected by IBIS/ISGRI, since we only observe the rise phase. We note the three bursts from SLX 1744-299 having E_b and y_b, which are on the edge of the ranges defined for intermediate bursts. Furthermore, Galloway & Keek (2017) state that all intermediate bursts reach the Eddington limit. This is not the case in any of the three bursts that we have observed from this source. Moreover, the bursts show a peculiar 'shoulder' at ≈60 per cent of the peak, and have prolonged tails, which could indicate hydrogen burning through rp-process (Heger et al. 2007). The nature of SLX 1744-299 and its peculiar bursts are out of the scope of this study, but they will be revisited in future work.

6.2 Enhanced persistent emission

The variable persistent flux method or f_a method for simplicity has been a standard method for analysing regular Type I X-ray bursts since 2015 (Worpel, Galloway & Price 2013; Worpel, Galloway & Price 2015). The procedure can be described as follows; (i) a pre-burst spectrum is obtained to model the accretion mission; (ii) parameters from the persistent emission model are included in the burst spectral fits and kept fixed at the values obtained from the fit of the pre-burst spectrum; and (iii) the persistent emission is multiplied with a variable normalization factor f_a. The f_a method has been tested for both PRE- and non-PRE regular bursts. The physical interpretation of the f_a factor is still a cause of debate, but an increase in the mass accretion rate is likely due to the effects of Poynting–Robertson drag on the disc material (Worpel et al. 2013).

Degenaar et al. (2016) applied a linear unsupervised decomposition method [non-negative matrix factorization (NMF)] to study a burst from 4U 1608-52, observed with *NuSTAR*. The main conclusion of the NMF method was a spectral softening of the persistent emission, which Degenaar et al. (2016) ascribed to the cooling of a corona.

We apply the same method to the bursts from our sample, for which we have detectable persistent emission. The TRSAs presented in Section 5.8.3 are not obtained using the f_a method, because the quality of our fits is not significantly improved, due to the poor spectral resolution.

Nevertheless, the f_a factor shows structure with an enhanced persistent emission in the peak and tail of bursts, which is comparable to the structure of regular bursts, reported by Worpel et al. (2013, 2015) and Degenaar et al. (2016). Furthermore, we see the persistent emission increase by a higher value of the f_a factor, ≈22 and ≈6, for a low-accreting source like SLX 1744-299, while the high-accreting sources like GX 17+2 and GX 3+1 show a dampened increase of the persistent emission (see Fig. 14). We are not able to apply the f_a method on three of the five PRE bursts in our sample, since their persistent emission level is below the threshold of the instrument. For the remaining two PRE bursts, the f_a factor remains nearly constant at ≈1.

The indicative structure of the f_a factor, mentioned above, justifies a deeper study of the enhanced persistent emission during long-duration X-ray bursts observed in instruments at higher spectral resolution.

7 CONCLUSION

We have performed a systematic analysis (using the same absorption model TBABS and the same energy binning) of all intermediate-duration X-ray bursts observed with the JEM-X instrument onboard the *INTEGRAL* satellite. With this study, we provide 13 bolometric light curves, which are suitable for comparison with numerical models. In particular, the bolometric light curves can be fitted to cooling models, and thereby provide a constraint on the energy release and ignition depth, independent of the recurrence time. This work is currently underway, and will soon be published elsewhere.

As for the eight previously reported bursts, our analysis reveals more clear indications of all three bursts from SAX 1737-282 being PRE bursts, where previously only one was identified as a PRE (Falanga et al. 2008), the first ever TRSA of the long burst from IGR J17254-3257 has been possible, and we have in general increased the number of time intervals, thereby increasing the resolution of the TRSAs.

From the new bursts, we identify one PRE with a relative strong expansion from AX J1754.2-2754, and we report three bursts from the UCXB candidate SLX 1744-299 (in't Zand et al. 2004), which show a peculiar 'shoulder' around ≈60 per cent of the peak and none of these show a PRE.

We apply the f_a method on five of the bursts in our sample, for which we had a reasonable persistent emission spectrum. This does not improve our fits, but shows an indicative structure of the f_a factor.

ACKNOWLEDGEMENTS

We are grateful to all the authors of the published work, which has been reanalysed for this study, for their support.

Lastly, we would like to convey our sincere thank you to Nathalie Degenaar from the Anton Pannekoek Institute for Astronomy, University of Amsterdam, Amsterdam, Jean in't Zand from SRON, Utrecht, and Erik Kuulkers from ESA/ESTEC, AZ Noordwijk. The fruitful discussions we had with both of them in the last phases of this study have been pivotal for this work.

This work is based on the long-term observations performed by the *INTEGRAL* international astrophysical gamma-ray observatory and retrieved via the Russian and European *INTEGRAL* Science Data Centers.

REFERENCES

Arnaud K. A., 1996, in Jacoby G. H., Barnes J., eds, ASP Conf. Ser. Vol. 101, Astronomical Data Analysis Software and Systems V. Astron. Soc. Pac., San Francisco, p. 17
Band D., Ferrara E., 2009, CICERONE: Detailed Manual for the Fermi Science Tools. NASA/GSFC, Greenbelt, MD, USA
Brown A. G. A. et al, 2018, A&A, 616, A1
Chelovekov I. V., Grebenev S. A., 2007, Astron. Lett., 33, 789
Chenevez J. et al., 2006, A&A, 449, L5
Chenevez J. et al., 2007, A&A, 469, L27
Chenevez J. et al., 2011, Astron. Telegram, 3183
Chernyakova M. et al., 2015, IBIS Analysis User Manual. ISDC, Versoix, Switzerland
Cornelisse R., Heise J., Kuulkers E., Verbunt F., in't Zand J. J. M., 2000, A&A, 357, L21
Cumming A., Bildsten L., 2000, ApJ, 544, 453
Cumming A., Bildsten L., 2001, ApJ, 559, L127
Cumming A., Macbeth J., 2004, ApJ, 603, L37
Cumming A., Macbeth J., in't Zand J., Page D., 2006, ApJ, 646, 429
Degenaar N., Koljonen K. I. I., Chakrabarty D., Kara E., Altamirano D., Miller J. M., Fabian A. C., 2016, MNRAS, 456, 4256
Falanga M., Chenevez J., Cumming A., Kuulkers E., Trap G., Goldwurm A., 2008, A&A, 484, 43
Fujimoto M. Y., Hanawa T., Miyaji S., 1981, ApJ, 247, 267
Galloway D. K., Keek L., 2017, preprint (arXiv:1712.06227)
Grindlay J., Gursky H., Schnopper H., Parsignault D. R., Heise J., Brinkman A. C., Schrijver J., 1976, ApJ, 205, L127
Hansen C. J., van Horn H. M., 1975, ApJ, 195, 735
Heger A., Cumming A., Galloway D., Woosley S. E., 2007, ApJ, 671, L141
in't Zand J. J. M., 1992, Ph.D Thesis, Univ. Utrecht
in't Zand J. J. M., Heise J., Bazzano A., Cocchi M., Smith M. J. S., 1999, IAU Circ., 7243, 2
in't Zand J. J. M., Cornelisse R., Cumming A., 2004, A&A, 426, 257
in't Zand J. J. M., Cumming A., van der Sluys M. V., Verbunt F., Pols O. R., 2005, A&A, 441, 675
in't Zand J. J. M., Jonker P. G., Markwardt C. B., 2007, A&A, 465, 953
Jager R. et al., 1997, A&A, 125, 557
Keek L., in't Zand J. J. M., Kuulkers E., Cumming A., Brown E. F., Suzuki M., 2008, A&A, 479, 177
Kuulkers E., 2002, A&A, 383, L5
Kuulkers E., 2004, Nucl. Phys. B, 132, 466
Kuulkers E., 2011, JEM-X Observer's Manual. ESA/ESAC, Madrid, Spain
Kuulkers E., van der Klis M., Oosterbroek T., van Paradijs J., Lewin W. H. G., 1997, MNRAS, 287, 495
Kuulkers E., Homan J., van der Klis M., Lewin W. H. G., Méndez M., 2002, A&A, 382, 947
Kuulkers E. et al., 2003, A&A, 399, 663
Kuulkers E. et al., 2010, A&A, 514, A65
Lewin W. H. G., van Paradijs J., Taam R., 1993, Space Sci. Rev., 62, 223
Lund N. et al., 2003, A&A, 411, L231
Maraschi L., Cavaliere A., 1977, in van den Heuvel E. P. J., ed., X-ray binaries and Compact Objects, Joint Discussion at the XVIth General Assembly of the I.A.U., Grenoble, 1976. p. 999
Markwardt C. B., Barthelmy C. D., Cummings J. C., Hullinger D., Krimm H. A., Parsons A., 2007, The SWIFT BAT Software Guide. NASA/GSFC, Greenbelt, MD, USA
Markwardt C. B., Altamirano D., Swank J. H., in't Zand J., 2008, Astron. Telegram, 1460
Molkov S., Revnivtsev M., Lutovinov A., Sunyaev R. A., 2005, A&A, 434, 1069
Oosterbroek T., Barret D., Guainazzi M., Ford E. C., 2001, A&A, 366, 138
Pavlinsky M. N., Grebenev S. A., Sunyaev R. A., 1994, ApJ, 425, 110
Sakano M., Koyama K., Murakami H., Maeda Y., Yamauchi S., 2002, ApJS, 138, 19
Savchenko V., Chernyakova M., Paizis A., Pavan L., Neronov A., Lecoeur-Taibi I, Türler M., 2018, The IBIS BAT Analysis User Manual. ISDC, Chemin d'Écogia, Switzerland
Seifina E., Titarchuk L., 2012, ApJ, 747, 99
Sguera V., Bazzano A., Bird A. J., 2007, Astron. Telegram, 1340
Skinner G. K., Willmore A. P., Eyles C. J., Bertram D., Church M. J., 1987, Nature, 330, 544
Strohmayer T. E., Bildsten L., 2006, in Lewin W., van der Klis M., eds., Compact Stellar X-ray Sources. Cambrigde Univ. Press, Cambrigde
Swank J. H., Becker R. H., Boldt E. A., Holt S. S., Pravdo S. H., Serlemitsos P. J., 1977, ApJ, 212, L73
Walter R., Bodaghee A., Barlow E. J., 2004, Astron. Telegram, 229
Westergaard N. J. et al., 2003, A&A, 411, L257
Worpel H., Galloway D., Price D. J., 2013, ApJ, 772, 94
Worpel H., Galloway D., Price D. J., 2015, ApJ, 801, 60

APPENDIX: LIGHT CURVES

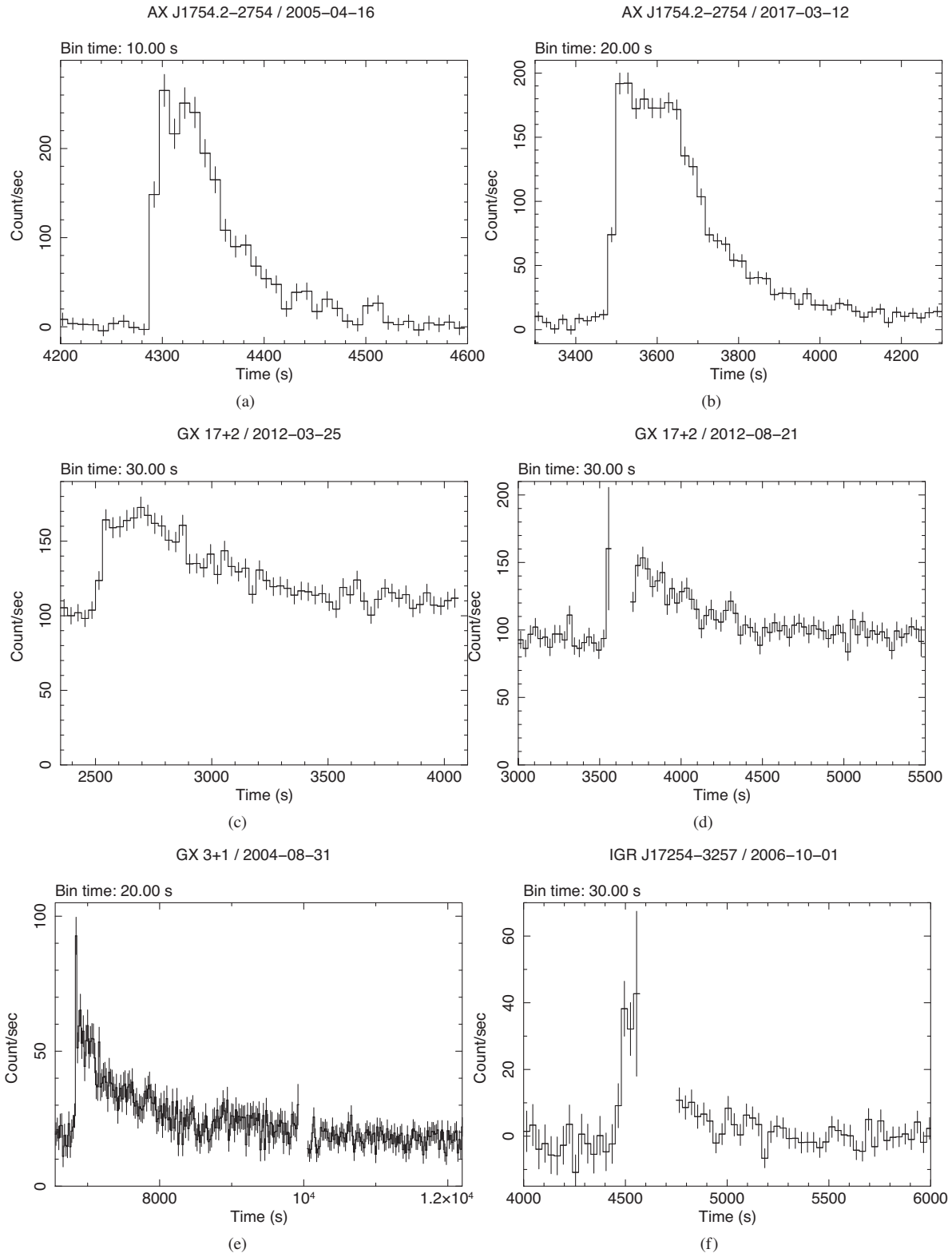

Figure A1. Light curves of the X-ray bursts investigated in this study.

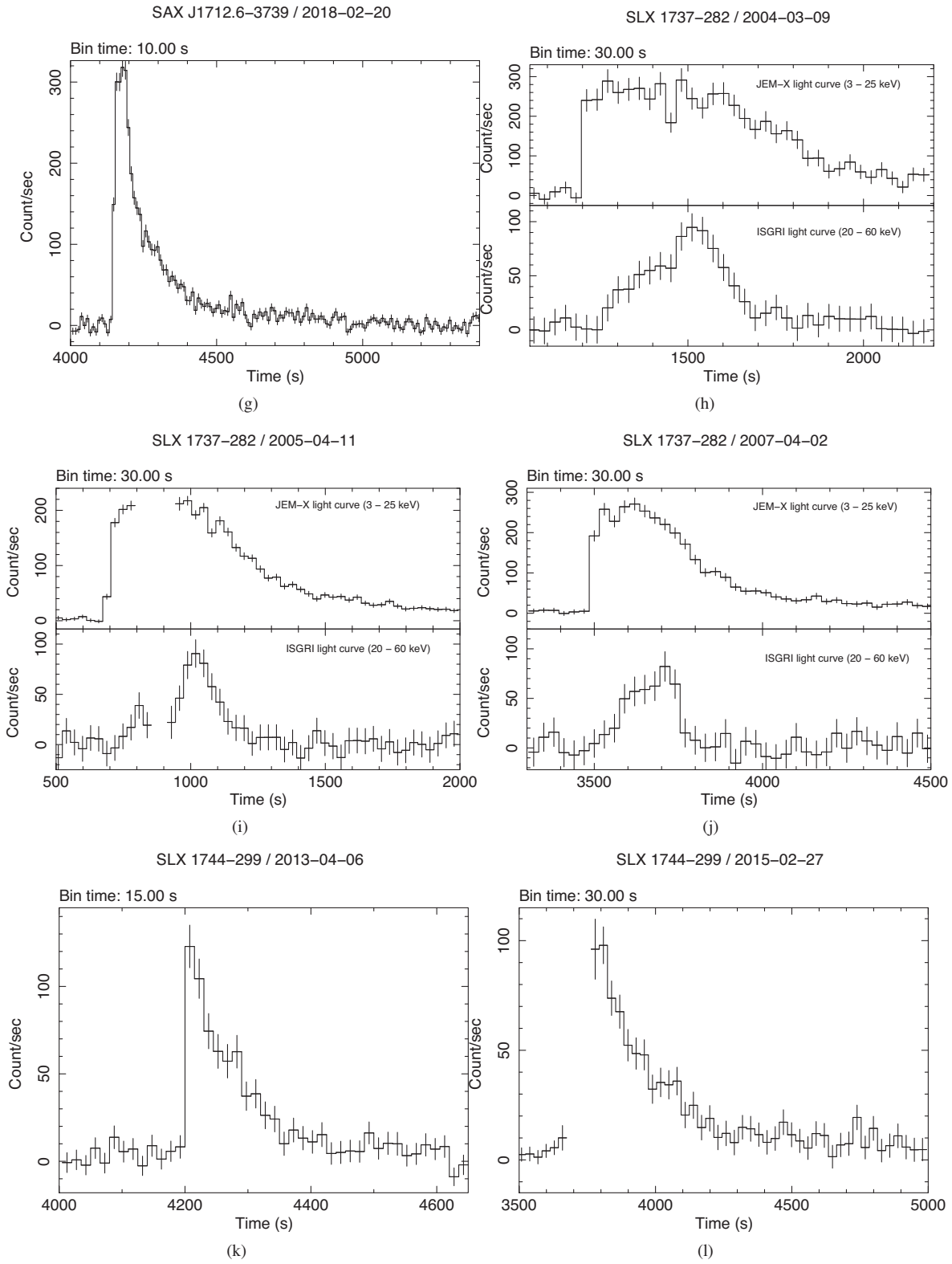

Figure A1 – *continued*

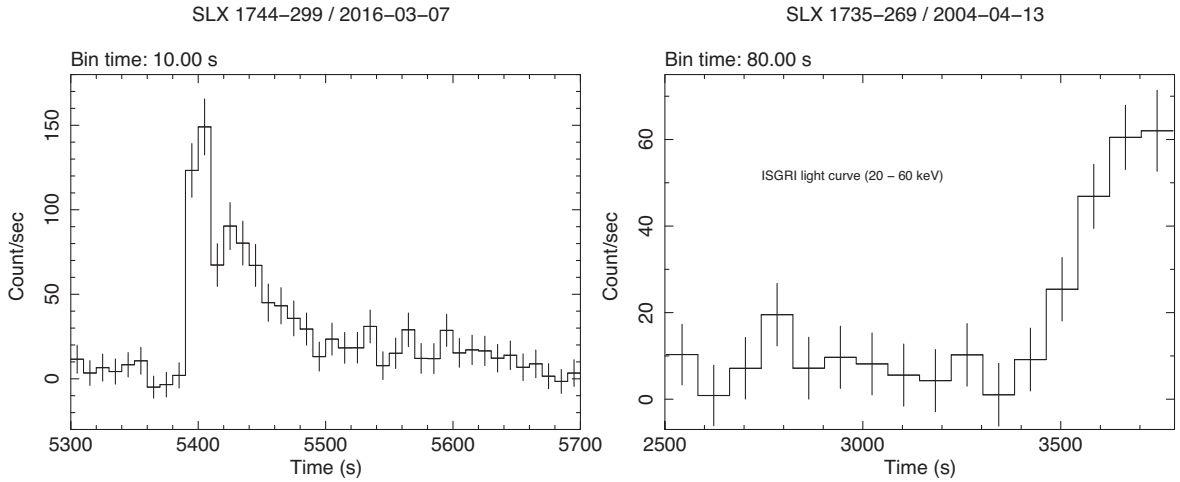

Figure A1 *– continued*

This paper has been typeset from a TEX/LATEX file prepared by the author.